

MIDI – THE 10 μ M INSTRUMENT ON THE VLT

CHRISTOPH LEINERT¹, UWE GRASER¹, FRANK PRZYGODDA¹,
LAURENS B.F.M. WATERS², GUY PERRIN³, WALTER JAFFE⁴, BRUNO LOPEZ⁵,
ERIC J. BAKKER⁴, ARMIN BÖHM¹, OLIVIER CHESNEAU¹,
WILLIAM D. COTTON⁶, SIEDS DAMSTRA⁷, JEROEN DE JONG⁴,
ANNELIE W. GLAZENBORG-KLUTTIG⁷, BERNHARD GRIMM¹,
HIDDO HANENBURG⁷, WERNER LAUN¹, RAINER LENZEN¹,
SEBASTIANO LIGORI¹, RICHARD J. MATHAR¹, JEFFREY MEISNER⁴,
SÉBASTIEN MOREL⁸, WERNER MORR¹, UDO NEUMANN¹, JAN-WILLEM PEL⁹,
PETER SCHULLER¹, RALF-RAINER ROHLOFF¹, BRINGFRIED STECKLUM¹⁰,
CLEMENS STORZ¹, OSKAR VON DER LÜHE¹¹ and KARL WAGNER¹

¹*Max-Planck-Institut für Astronomie, Heidelberg, Germany*

²*Astronomical Institute, University of Amsterdam, Netherlands*

³*DESPA, Observatoire de Paris-Meudon, France*

⁴*Sterrewacht Leiden, University of Leiden, Netherlands*

⁵*Observatoire de la Côte d'Azur, Nice, France*

⁶*NRAO, Charlottesville, Virginia, USA*

⁷*ASTRON, Dwingeloo, Netherlands*

⁸*ESO, Garching, Germany*

⁹*Kapteyn Observatory, University of Groningen, Netherlands*

¹⁰*Thüringer Landessternwarte Tautenburg, Germany*

¹¹*Kiepenheuer-Institut für Sonnenphysik, Freiburg, Germany*

Abstract. After more than five years of preparation, the mid-infrared interferometric instrument MIDI has been transported to Paranal where it will undergo testing and commissioning on the Very Large Telescope Interferometer VLT from the end of 2002 through large part of this year 2003. Thereafter it will be available as a user instrument to perform interferometric observations over the 8 μ m–13 μ m wavelength range, with a spatial resolution of typically 20 milliarcsec, a spectral resolution of up to 250, and an anticipated point source sensitivity of $N = 3$ –4 mag or 1–2.5 Jy for self – fringe tracking, which will be the only observing mode during the first months of operation. We describe the layout of the instrument, laboratory tests, and expected performance, both for broadband and spectrally resolved observing modes. We also briefly outline the planned guaranteed time observations.

Keywords: VLT, MIDI, interferometry, mid-infrared, thermal infrared

1. Introduction

Up to now, interferometry in the mid-infrared around 10 μ m has been performed only in narrow-band heterodyne operation. The quite successful ISI instrument (Bester et al., 1990) therefore is limited to rather bright objects of about 100 Jy or more. The mid-infrared interferometric instrument MIDI, covering the full 8



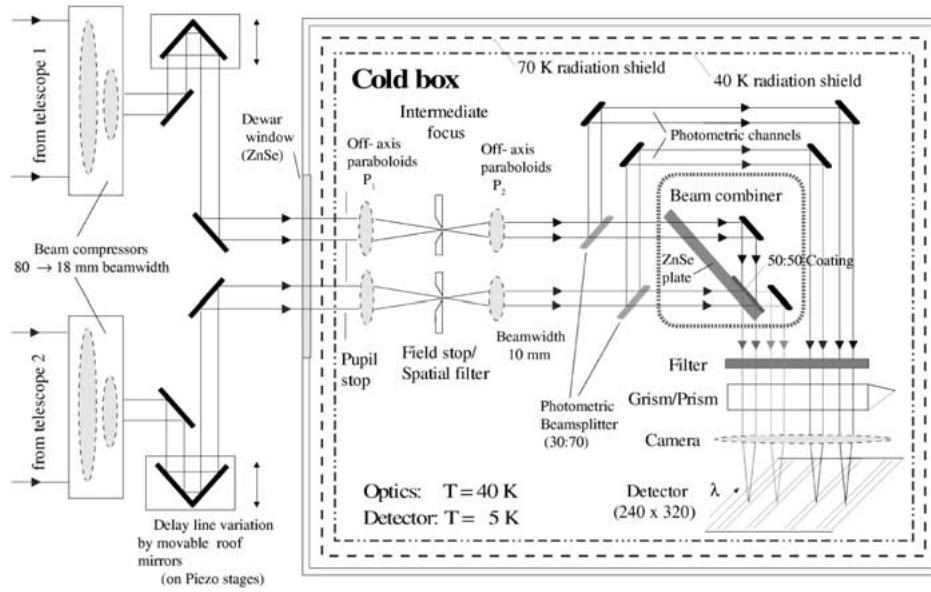


Figure 1. Optical concept of MIDI. Beams are called A (bottom) and B.

μm – $13 \mu\text{m}$ range of the N band, is one of the two first generation instruments of the Very Large Telescope Interferometer (VLTI), the second one, AMBER, working in the near-infrared. After successful commissioning MIDI will be the first instrument doing direct combination $10 \mu\text{m}$ interferometry worldwide. Its main advantage with respect to the ISI heterodyne interferometer will be the higher sensitivity, due both to the larger diameter telescopes of the VLTI and the ability for broadband operation. Observations of sources with brightness 1Jy ($N = 4 \text{ mag}$) appear possible initially, and a range of objects fainter by a factor of 10–100 should become accessible once external fringe stabilisation by a dedicated fringe tracker has been introduced at the VLTI.

2. Principle of Measurement

The design of the instrument has been driven by the necessity to suppress as well as reasonably possible the strong thermal emission from the environment (Figure 1). Most of the instrument optics have to be in a dewar and to be cooled to cryogenic temperatures $40 \pm 5 \text{ K}$ and to be surrounded by a wall at the same temperature in order not to disturb the detector by residual thermal emission. The detector itself operates at $5\text{--}10 \text{ K}$. A second radiation shield at about 77 K has to be introduced just inside the dewar walls to block the thermal radiation of the dewar housing. Good suppression of the thermal radiation of external background surrounding the field-of-view requires designing for both a cold pupil and a cold field stop

inside the instrument. We choose to have beam combination in (or close to) the reimaged pupil and to detect the signal in the image plane. This appeared to us the most practical and promising way to provide the baffling against the very high and varying thermal background and to reduce the effects of variable pixel responsivity.

The instrument has been built to combine the beams from two telescopes at a time, which gives the best sensitivity. In Figure 1, from the left the afocal beams from two telescopes of the VLTI are approaching the instrument. Their nominal diameter is 80 mm, and they are reduced to 18 mm diameter by a beam compressor provided as part of the VLTI infrastructure, represented here for simplicity by two lenses.

After the four folding mirrors of a small experiment-internal delay line, the compressed beams enter the cryostat (‘Cold box’) through the entrance window (‘Dewar window’). Each telescope pupil is imaged by the VLTI delay line optics onto a cold pupil stop to provide the needed suppression of thermal emission from outside the beams. Next, an intermediate focus is formed, where different slits or diaphragms (i.e. spatial filters) can be introduced for additional suppression of unwanted radiation. If no spatial filters are used, the detector pixels, which are much smaller than the image of the telescope Airy disk, provide an alternative and flexible way to limit the spatial region admitted for the measurement. Then the beams are recollimated (again, reflective optics are represented by lenses for simplicity) and move on to combine on the surface of a 50%:50% beam splitter. This coating is indicated on the lower back side of the ZnSe plate. Here is the heart of the instrument.

From the beam combiner onwards, the two interfering beams have a common optical axis. Actually, there are two of such overlaid beams, one outgoing to each side of the beam combiner. These two outputs are modulated in flux depending on the optical path difference of the interfering beams, but with opposite sense because of energy conservation.

We measure the degree of coherence between the interfering beams (i.e. the object visibility at the actual baseline setting) by artificially stepping the optical path difference between the two input beams rapidly over at least one wavelength within the coherence time of ≈ 0.1 s. This is done with help of the piezo-driven roof mirrors forming part of the small delay lines just outside the cryostat. The result in both channels is a signal modulated with time (‘temporal fringe’), from which the fringe amplitude can be determined. The large and not precisely known thermal background forces us to determine the total flux separately by a chopped measurement, chopping between the object and an empty region of the sky, and determining the source flux by subtraction. By dividing fringe amplitude by total flux the visibility is obtained.

The measured visibility gets reduced if the flux is not the same in the two incoming beams. For good accuracy of the visibility determination, the relative fluxes of the combining beams have to be known at the time of the fringe measurement. To this end, part of the incoming light can be extracted out of both of



Figure 2. MIDI in the interferometric laboratory on Paranal. The telescope beams come in from lower right, the cold optics are hidden in the almost cubic dewar housing in the back, and the warm optics in positioned on the optical table in front of it.

the incoming beams before beam combination, and these so-called ‘photometric beams’ or ‘photometric channels’ are also imaged onto the same detector and in the same way as the interferometric signal.

Spectral resolution is obtained by filters or with a prism or grism in the parallel beam after beam combination. This provides moderate spectral resolution and also can be used to keep the detector from saturating very quickly, within the order of 1 ms for a broad-band filter.

In principle, for the measurements with MIDI the full interferometric field of $\pm 1''$ is available simultaneously. This is a small area on the sky, but about 8 times larger than the FWHM of the Airy disk of a single telescope, to which interferometric measurements are normally limited. In any case, this available field helps to identify the objects on the telescope.

3. Realisation

The instrument realised according to this concept can be seen in Figure 2 at its final place in the interferometric laboratory of the VLTI on Paranal. Figures 3 and 4 show how the concept evolved to a design and finally to the instrument hardware. In particular the cold optics (Figure 4) came out quite compact. This is on purpose

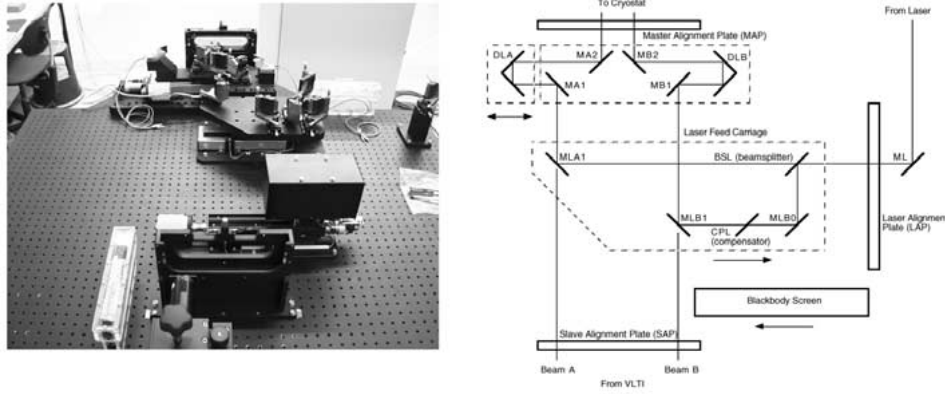


Figure 3. warm optics hardware and schematics

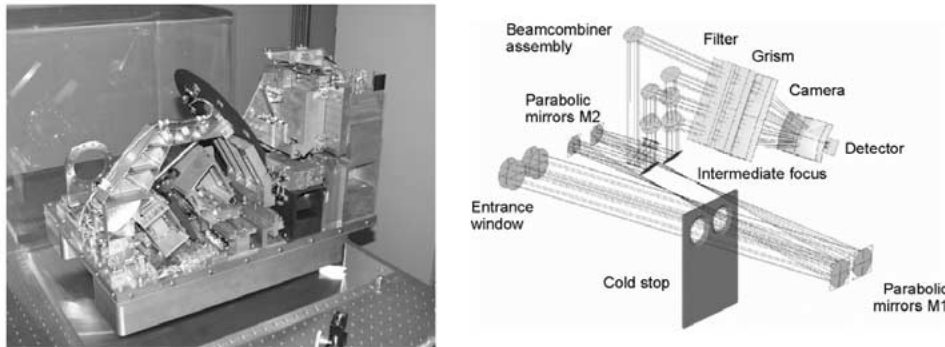


Figure 4. cold optics hardware and schematics

to keep internal flexures and vibrations at a low level (Glazenberg-Kluttig et al., 2003).

4. Options

For most of the optical elements, like field stops, cameras, filters, dispersing elements, the instrument provides flexibility by several choices, which are summarised in the following tabular presentation. Out of the many possible combinations only those most useful for actual observations will be offered, depending on the outcome of the commissioning runs. A future extension to observations at to 20 μ m is in preparation.

| | | |
|--------------------------------|-------------------------------------|--|
| cameras | field camera | $\lambda/D = 3$ pixels |
| | spectral camera | $\lambda/D = 1 \times 2$ pixels (1 in spectral direction, 2 in spatial direction) |
| | pupil camera | pupil diameter = 40 pixels |
| dispersing elements | grism | resolution per two pixels : 220 at $10 \mu\text{m}$ |
| | prism | resolution per two pixels: 35 at $10 \mu\text{m}$ |
| | none | for observations with filters |
| filters | 10 filters | including full N-band, short N band ($8.0\text{--}9.5 \mu\text{m}$), long N ($10.5\text{--}13.1 \mu\text{m}$), narrow bands |
| focal plane | no diaphragm | 2 mm diameter (oversized) |
| | full field | 1 mm diameter ($2.6''$ on UTs) |
| | slit width | $50 \mu\text{m}$, $100 \mu\text{m}$, $200 \mu\text{m}$ |
| | single pinhole | 0.4 mm diameter ($1.0''$ on UTs) |
| | triple pinholes, spacing 0.29 mm | $70 \mu\text{m}$, $110 \mu\text{m}$, $170 \mu\text{m}$ (diameter) |
| beamcombiner unit | high sensitivity | no photometric beams |
| | with photometric beam extraction | 30 % of light goes to photometric channels |
| | open | no beam combination |

5. Observing Modes

The observing modes of MIDI and the preparation for interferometric observations at mid-infrared wavelengths are the topic of a separate paper in these proceedings (Przygodda et al., 2003). Here, we give a short overview on how data will be taken with this instrument.

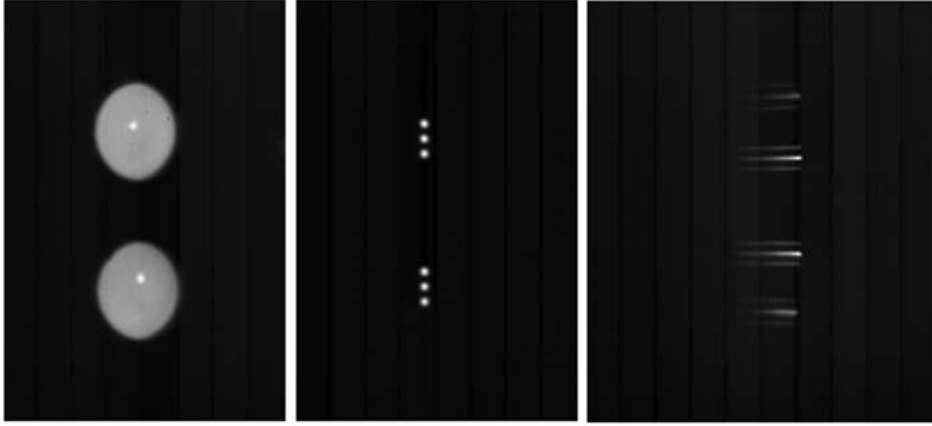


Figure 5. Typical examples for the light distribution on the detector. From left to right: point source in the open field which is filled by background radiation; triple pinholes illuminated by background radiation; prism with slit and triple pinholes and point source in the central pinhole (see text for details).

The detector is a Si:As impurity band conduction (IBC) array produced by Raethyon, 320×240 pixels in size. It is read out in 16 bands, each 20 pixels wide, which gives rise to the band structure weakly seen in the panels of Figure 5. The readout noise is ≈ 1000 electrons. The readout electronics, quite flexible, allow a full frame readout time of 5.6 ms, which time can be further reduced by reading only rows of relevance for the current observation (so-called ‘hardware windowing’). Standard operation is first to take the exposure, then to read out (‘integrate then read’). More details are given by Ligori et al. (2003).

The full long dimension of the detector is only used with the higher dispersion grism observations, its full height only when the photometric beams are extracted. For most observing modes only part of the detector array is illuminated, for which a few examples are shown in Figure 5. On the left, no diaphragm has been inserted in the focal plane. The thermal background radiation of the laboratory environment fills the field for the two incoming beams A and B (up), while a laboratory source – fed into both beams at the same time to simulate a star – produces the point-like bright spots. In the middle, a triple pinhole has been used for both beams with the laboratory source switched off. The illumination is due to the thermal background radiation, always strong at 10 μ m. A slit would occupy the same position as the triple pinholes. On the right, the triple pinhole has been used again and the prism has been inserted. The dispersed spectrum has the short wavelengths on the right end. In each case, the middle spectrum is the brightest, because the laboratory source has been centered on the middle one of the triple pinholes. The separation in vertical direction is smaller than in the two first panels because the spectroscopic camera with its shorter focal length has been used here. Finally, for these measure-

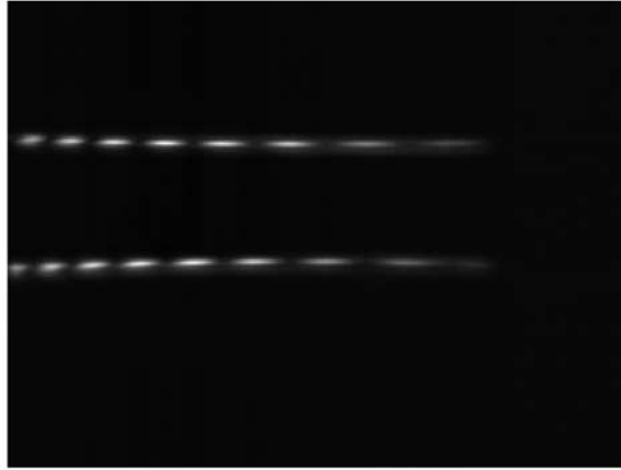


Figure 6. Dispersed fringes measured in the laboratory. The optical path difference between the two interfering beams was about $140\ \mu\text{m}$.

ments the photometric beams have been extracted by inserting a beam splitter. This leads to the two additional spectra on the top and bottom of the panel.

Interference patterns for determination of source visibility are produced in two ways. For undispersed data, the optical path difference (OPD) between the two input beams is varied by moving one of the roof mirrors of the small internal delay line. This results in a fringe pattern, which is damped according to the width of the filter used (see example in Przygodda et al., 2003). For dispersed data, the OPD is offset on purpose from zero by several wavelengths. Then the fringe pattern appears at any instant as a modulation of the spectrum with wavelength (Figure 6).

6. Anticipated Performance

While the obtainable spatial resolution is given by the geometrical arrangement of the telescopes of the VLTI and the wavelength of observation, the sensitivity of the instrument is determined mostly by the properties of the atmosphere. First, the thermal emission of the VLTI mirror train of about 2×10^{11} photons per s per Airy disk results in a correspondingly high photon noise against which the signals have to be detected. Second, the integration is limited to about 0.1 s, since the fringe motion due to the turbulent atmosphere would smear the fringe pattern at substantially longer integration times. It still has to be proven that fluctuations of sky brightness are of lower importance compared to background photon noise and that the assumed integration times are available. However, the given estimates of limiting magnitude for self-fringe-tracking operation are based on this assumption.

The sensitivity of the instrument can be increased if external stabilisation of the fringes is provided, which should become available on the VLTI within the coming

TABLE I
Basic parameters of the MIDI instrument

| | | |
|--|---|------------------------------------|
| Telescope diameter | UTs | 8 m |
| | ATs | 1.8 m |
| Baselines available | UTs | 47 ... 130 m |
| – one at a time | ATs | 8 ... 200 m |
| Resolution | λ / D for 100 m | 0.020'' at 10 μ m |
| Wavelength coverage | | N band (8 μ m–13 μ m) |
| | expandable to | Q band (17 μ m–26 μ m) |
| Field of view | UTs | $\pm 1''$ |
| | ATs | $\pm 5''$ |
| Airy disk (FWHM at 10 μ m) | 8 m telescopes | 0.26'' |
| | 1.8 m telescopes | 1.14'' |
| Input beam diameter | from UTs | compressed to 18 mm |
| | from ATs | 18 mm |
| Throughput of VLTI | to instrument | 30 %–35 % |
| Sampling time for fringe measurement | for fringe motion $\leq 1 \mu$ m rms | 100 ms |
| Atmospheric stability | for chopping | 200 ms |
| Background (in Airy disk) | from sky | $2 \cdot 10^{10}$ photons/sec |
| | from VLTI | $2 \cdot 10^{11}$ photons/sec |
| Detector(320 \times 240 pixels) | full well capacity | $\approx 1.0 \cdot 10^7$ electrons |
| | read noise | ≤ 1000 electrons |
| Limiting N-magnitude (self-fringe tracking) | UTs | 3–4 mag (1–2.5 Jy) |
| | ATs | 0–0.8 mag (20–50 Jy) |
| Limiting N-magnitude (external fringe tracking) | UTs | 8–9 mag (10–25 mJy) |
| | ATs | 5–5.8 mag (200–500 mJy) |
| Accuracy of visibility | | $\pm 5 \%$ |
| Phase measurement | internally | differential within band |
| | external referencing | possible |

year. Then the fringe patterns of individual short observations can be added blindly and coherently, and theoretically a gain proportional to square root of integration time could be obtained. By adding up 10^4 individual 100 ms integrations this could improve the limiting magnitude by up to 5 mag. The sensitivities given in Table I refer to the use of the full N band. For spectrally dispersed measurements with the grism, the limiting magnitudes will be reduced by 1–1.5 mag.

7. Scientific Programme

The scientific potential of the MIDI instrument has been discussed by Lopez et al. (2000). Based on the slightly optimistic sensitivity estimates of the preceding section, a guaranteed time programme has been selected to fill the 300 hours of guaranteed observing time available to the instrument team on the UTs. This listing gives an impression what may be feasible to observe with the MIDI instrument. It has to be kept in mind that the attempt for direct planet detection is untypical. It is a programme of extremely high risk for possibly high reward.

The actual observations on the VLTI will be performed in the form of so-called ‘observation blocks’ and with procedures described for the case of observations with MIDI by Bakker et al. (2003).

| Topic | Telescopes | |
|---|------------|-------|
| | UTs | ATs |
| Dust Tori in Nearby Active Galactic Nuclei | 65 h | – |
| Inner disks of low-mass young stellar objects | 65 h | 90 h |
| Inner disks around intermediate-mass young and Vega-type stars | 62.5 h | 100 h |
| Massive young stars | 52.5 h | 305 h |
| The dusty environment of hot stars | 2 h | 68 h |
| Cool Late Type Stars and related objects | 25 h | 450 h |
| Extra-solar planets and brown dwarfs | 25 h | – |

8. Next Steps for 10 μ m Interferometry with MIDI

First observing runs on the baseline UT1-UT3, in self-fringe-tracking mode and therefore limited to brighter objects have started in the summer of 2003. After this the following development steps are foreseen:

- Fall of 2003 – additional UT baselines
 – adaptive optics, external fringe tracking,
 allowing to go to fainter sources
- Spring of 2004 – observations with the 1.8 m telescopes
 (ATs) of the auxiliary array
- Fall of 2004 – extension to 20 μ m observations
 – addition of 10 μ m single mode fiber
 in the focal plane for beam cleaning
- 2005 – dual-beam capability on the VLTI,
 allowing to observe faint sources

With these added possibilities, MIDI should become an instrument applicable to a wide range of astronomical studies.

Acknowledgements

We thank the electronic and mechanical workshops in Heidelberg, Dwingeloo and Freiburg for their accurate and careful work, without which the instrument would not have become reality. And we thank the instrument responsables at ESO, Markus Schöller, Andrea Richichi and Peter Biereichel, for positively critical partnership.

References

- Bakker, E.J., Przygodda, F., Chesneau, O. and Jaffe, W.: 2003, *MIDI* scientific and technical observing modes, *SPIE* **4838**, 905–916.
- Bester, M., Danchi, W.C. and Townes, C.H.: 1990, Long baseline interferometer for the mid-infrared, *SPIE* **1237**, 40–48.
- Glazeborg-Kluttig, A.W., Przygodda, F., Hanenburg, H., Morel, S., Pel, J.-W.: 2003, *Realization of the MIDI Cold Optics*, *SPIE* **4838**, 1171–1181.
- Ligori, S., Graser, U., Grimm, B. and Klein, R.: 2002, in: Kona, W. Traub (ed.), *Experiences with the Raethyon Si:As IBC Detector Arrays for Mid-IR Interferometric Observations*, *SPIE* **4838**, 774–785.
- Lopez, B., Leinert, Ch., Graser, U. et al.: 2000, The astrophysical potentials of the MIDI VLTI instrument, *SPIE* **4006**, 54–67.
- Przygodda, F., Chesneau, O., Graser, U., Leinert, Ch. and Morel, S.: 2003, Interferometric observations at mid-infrared wavelengths with MIDI, these proceedings,

